

## Seepage analysis of earth dams considering spatial variability of hydraulic parameters



Xiaohui Tan<sup>a,b,\*</sup>, Xue Wang<sup>a</sup>, Sara Khoshnevisan<sup>c</sup>, Xiaoliang Hou<sup>a</sup>, Fusheng Zha<sup>a</sup>

<sup>a</sup> School of Resources and Environmental Engineering, Hefei University of Technology, Hefei 230009, China

<sup>b</sup> Glenn Department of Civil Engineering, Clemson University, Clemson, SC 29634, United States

<sup>c</sup> Department of Civil and Environmental Engineering, Clarkson University, Potsdam, NY 13699, United States

### ARTICLE INFO

#### Keywords:

Seepage  
Spatial variability  
Autocorrelation  
Dam  
Monte Carlo simulation  
van Genuchten model

### ABSTRACT

To investigate the influence of spatial variability of hydraulic parameters on the flow in earth dams, saturated-unsaturated seepage is numerically simulated combining Monte Carlo simulation and random field theory. The van Genuchten model is adopted to represent soil-water characteristic curve (SWCC). The SWCC fitting parameters ( $\alpha$ ,  $n$ ) and the saturated hydraulic conductivity parameter ( $k_s$ ) are considered as lognormal random fields. An approach of logarithmic translation is used for generating lognormal variables with lower limits greater than zero. The influence of the coefficient of variation (COV) and autocorrelation distance of hydraulic parameters on the flow rate is studied and compared. Sensitivity analysis indicates that the COVs of SWCC parameter  $n$  and saturated hydraulic conductivity  $k_s$  have a larger effect on the flow rate than that of SWCC parameter  $\alpha$ . A larger horizontal autocorrelation distance corresponds to a larger mean and COV of the flow rate. Neglecting the spatial variability of hydraulic parameters leads to overestimation of the mean and COV of the flow rate in earth dams, which could lead to conservative design of dams.

### 1. Introduction

Accurate analysis of seepage process is essential in many applications in geotechnical engineering. The study of saturated-unsaturated seepage is of particular interest because the distribution of matric suction in both the saturated and unsaturated zones influences flow rates, shear strength and stability of geotechnical structures. Modeling unsaturated flow is very difficult as the hydraulic conductivity of unsaturated soil depends on degree of saturation, and the degree of saturation depends on suction. The relationship between hydraulic conductivity and suction is nonlinear. Therefore, numerical simulations are needed for solving unsaturated seepage problems. With the development of computing technology, many authors began to investigate unsaturated seepage problems in dams and/or soil slopes (van Genuchten, 1980; Cho and Lee, 2001; Tsaparas et al., 2002; Rahimi et al., 2010; Kim et al., 2012).

Most geotechnical analyses which adopt deterministic approaches are based on the assumption that soil properties are deterministic values. However, many uncertainties exist in soils due to different deposition environments and measurement errors. Extensive studies have been carried out in geotechnical engineering to investigate the influence of parameter uncertainties on the stability, seepage or deformation

(Babu and Murthy, 2005; Lu et al., 2009; Juang et al., 2009, 2012, 2014; Tan et al., 2011; Chan and Low, 2012; Wang et al., 2013, 2015). In these probabilistic studies, geotechnical parameters are often considered as random variables.

It is well known that soil properties often vary significantly from point to point as a result of depositional and post-depositional processes. Traditional probabilistic approaches cannot reflect the spatial variability of soil properties. Random field theory is an effective tool for modeling the spatial variability of soil parameters (Vanmarcke, 1977). In a random field, variables exhibit autocorrelation, which is a tendency for soil properties at one point to be correlated to soil properties at nearby points. The spatial continuous variable in a random field should be discretized into a sequence of values at different points (Qin et al., 2006). The discrete values are mapped onto finite element or finite difference mesh as input soil parameters for the numerical modeling of seepage analysis. Monte Carlo simulation method (MCSM) is usually adopted to perform stochastic simulations of seepage across saturated and unsaturated regions of heterogeneous soil for investigating the statistical characteristics of computed flow responses (Le et al., 2012; Cho, 2012; Gui et al., 2000).

Saturated-unsaturated flow depends on the hydraulic conductivity of unsaturated soil, which is a function of saturated hydraulic

\* Corresponding author.

E-mail address: [tanxh@hfut.edu.cn](mailto:tanxh@hfut.edu.cn) (X. Tan).

conductivity and curve fitting parameters of soil water characteristic curve (SWCC). SWCC is a very important curve for unsaturated soil because it can reflect the relationship between matric suction and water content or the degree of saturation. Many fitting models have been proposed for SWCC (Nam et al., 2009; Sillers and Fredlund, 2001). Phoon et al. (2010) demonstrated that the variability of SWCC parameters is large and has significant impact on unsaturated seepage and slope stability. In the stochastic analysis of earth dams or slopes, many studies considered only the spatial variability of saturated hydraulic conductivity ( $k_s$ ), and lognormal distribution was assumed for it (Ahmed, 2009; Gui et al., 2000; Cho, 2012; Zhu et al., 2013). Recently, some other parameters were also considered as random fields. For example, Le et al. (2012) considered porosity ( $n_p$ ) as a random field, and thus the random fields of the saturated hydraulic conductivity ( $k_s$ ) and a SWCC parameter ( $s_e$ ) were generated by a functional relationship between  $k_s$  or  $s_e$  and  $n_p$ . Li et al. (2009) considered three hydraulic parameters as random fields to test the capacity of probabilistic collocation method.

From the literature review, it emerges that the uncertainty in soil properties affects the saturated-unsaturated flow significantly. However, few attempts have been made to study the effect of the uncertainties of both the saturated hydraulic conductivity and SWCC parameters to the flow through saturated and unsaturated zones. The objective of this paper is to investigate the influence of spatial variability of hydraulic parameters on the flow in a heterogeneous soil dam. Spatial variability of the saturated hydraulic conductivity and two SWCC parameters are taken into account by considering them as correlated lognormal random fields (Phoon et al., 2010; Wang et al., 2015). The van Genuchten model is used for describing soil-water characteristics. Monte Carlo simulation combined with finite difference method is used for investigating the statistics of the flow rate. Furthermore, the influence of the coefficients of variation and the autocorrelation distances on flow rate are studied and compared.

## 2. Saturated-unsaturated seepage analysis

Soil is a porous material which includes soil particles and voids. A soil is saturated when the voids are completely filled with water phase. And when the voids are filled with both water phase and air phase, the soil is unsaturated. For the unsaturated soil, relationship between the saturation of water phase ( $S_w$ ) and air phase ( $S_a$ ) is:  $S_w + S_a = 1$ .

Seepage in unsaturated soils is very complicated because it is affected by matric suction, water content, saturation, permeability, particle size, and etc. For the analysis of saturated-unsaturated seepage process, soil-water characteristic curve (SWCC) and hydraulic conductivity function are needed.

Soil-water characteristic curves (SWCCs) give the relationship between matric suction (hereinafter referred to as suction) and the degree of saturation. They have been used extensively for the estimation of unsaturated soil properties (Fredlund and Houston, 2009). According to the SWCC fitting model proposed by van Genuchten (1980), the effective degree of saturation ( $S_e$ ) can be expressed as:

$$S_e = \frac{1}{(1 + (\psi/a)^n)^m} \quad (1)$$

where  $\psi = u_a - u_w$  is the suction,  $u_a$  and  $u_w$  are pore air pressure and pore water pressure, respectively;  $a$ ,  $n$  and  $m$  are curve fitting parameters and  $m = 1 - 1/n$ . It should be noted that the value of  $m$  cannot be negative and therefore the value of  $n$  cannot be less than 1.0. Parameter  $a$  is a suction value corresponding to the inflection point on the SWCC which is larger than the air entry value. Although it does not affect the shape of the curve, it shifts the curve toward the higher or lower suction regions of the plot. Parameter  $n$  is related to the rate of change of the desaturation zone of the SWCC (Sillers and Fredlund, 2001). Note that parameter  $m$  is not an independent variable due to the fixed relationship between  $n$  and  $m$ .

Hydraulic conductivity function gives the relationship between suction (or degree of saturation) and the hydraulic conductivity of unsaturated soils. Denoting the hydraulic conductivity of water phase and air phase as  $k^w$  and  $k^a$ , respectively, therefore  $k^w$  and  $k^a$  are related to the effective saturation by empirical laws of the van Genuchten form (van Genuchten, 1980):

$$k^w = k_s S_e^{0.5} [1 - (1 - S_e^{1/m})^m]^2 \quad (2)$$

$$k^a = k_s (1 - S_e)^{0.5} (1 - S_e^{1/m})^{2m} \quad (3)$$

From Eqs. (1) to (3), the uncertainty of hydraulic conductivity of fluid phases are characterized by the uncertainty of two curve fitting parameters of SWCC (i.e.  $a$  and  $n$ ) and saturated hydraulic conductivity  $k_s$ . Thus, the hydraulic conductivity function varying from one point to another can be represented by three random fields of  $a$ ,  $n$  and  $k_s$ .

## 3. Discretization of random fields

### 3.1. Theory of random field

Early probabilistic analysis of geotechnical engineering typically modeled the material uncertainties using random variables for the whole profile without including spatial variability. Vanmarcke (1977) suggested that random field models could be used to describe the spatial variability of soil properties. Random variables that vary continuously over a space domain are referred to as random fields. In a random field, the variable exhibits autocorrelation, which is the tendency for values of the variable at one point to be correlated to values at nearby points. To characterize a random field, the mean, standard deviation (or coefficient of variation) and autocorrelation function are required. The correlation function models the reduction in autocorrelation with distance. Autocorrelation functions commonly used in geotechnical engineering have been presented by many authors (Qin et al., 2006; Jiang et al., 2014). In this study, an exponential autocorrelation function is used (Jiang et al., 2014):

$$\rho_A(\tau_x, \tau_y) = \exp\left(-\frac{\tau_x}{L_h} - \frac{\tau_y}{L_v}\right) \quad (4)$$

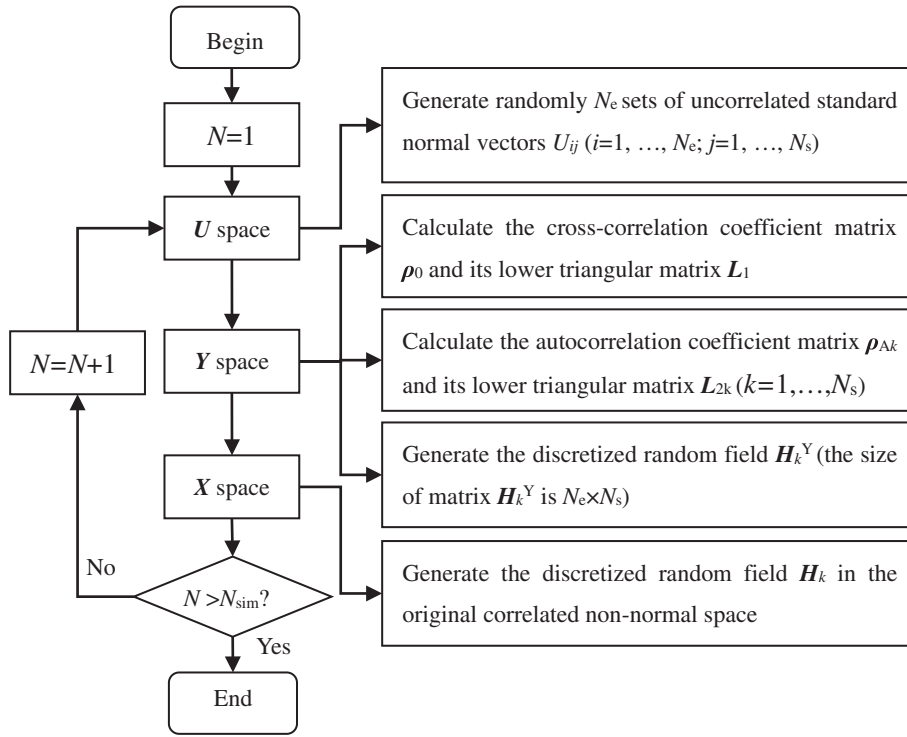
where  $\rho_A$  is the autocorrelation coefficient of two points in space, whose horizontal and vertical absolute distances are  $\tau_x$  and  $\tau_y$ , respectively;  $L_h$  and  $L_v$  are the horizontal and vertical autocorrelation distances, respectively. A large autocorrelation distance value implies that the soil property is highly correlated over a large spatial extent, and a small autocorrelation distance value indicates that the fluctuation of the soil property is large (Stefanou, 2009).

### 3.2. Discretization of cross-correlated non-normal random fields

Because of the discrete nature of numerical methods such as finite element or finite difference formulation, a continuous-parameter random field must be discretized into random variables. This process is commonly known as discretization of a random field. Many methods have been developed to perform this task. The discretization methods can be mainly split into three categories: point discretization methods, average-type discretization methods, and series expansion methods (Sudret and Kiureghian, 2002; Ji et al., 2012). Although the point discretization methods are not as efficient as the series expansion methods, they are still widely used due to simplicity and straightforward implementation (Cho, 2007; Papaioannou and Straub, 2012; Ching and Phoon, 2013; Jiang et al., 2014). Therefore, midpoint method, one type of point discretization method, is adopted in this study to discretize random fields of soil hydraulic properties. In the midpoint method, the value of a random field over each element is represented by its value at the midpoint of that element.

Consider  $N_s$  cross-correlated non-Gaussian random fields. Define the number of discretization points of random fields as  $N_e$ , which is equal to

Fig. 1. Flowchart of midpoint discretization method.



the number of finite elements in the numerical analysis. Thus, the size of cross-correlation coefficient matrix of  $N_s$  random fields,  $\rho$ , is  $N_s \times N_s$ ; and the size of autocorrelation coefficient matrix of the  $k$ -th random field,  $\rho_{Ak}$ , is  $N_e \times N_e$ , where  $k = 1, \dots, N_s$ . Denote the uncorrelated standard normal space, correlated standard normal space, and correlated non-normal space as  $U$  space,  $Y$  space and  $X$  space, respectively. The main processes of the discretization of cross-correlated non-normal random fields by the midpoint discretization method are summarized in Fig. 1.

Fig. 1 shows the flowchart of the midpoint discretization method. The main steps are explained as follows:

- (1) Uncorrelated standard normal space ( $U$  space): A matrix of sample points  $U$ , whose size is  $N_e \times N_s$ , is generated randomly.
- (2) Correlated standard normal space ( $Y$  space): The cross-correlation coefficient matrix  $\rho_0$  (whose size is  $N_s \times N_s$ ) in  $Y$  space can be calculated based on the cross-correlation coefficient matrix  $\rho$  in  $X$  space, and the autocorrelation coefficient matrix  $\rho_{Ak}$  ( $k = 1, \dots, N_s$ ) can be calculated according to Eq. (4). For lognormal random variables, the relationship between  $\rho_0$  and  $\rho$  can be expressed as (Jiang et al., 2014):

$$\rho_{0ij} = \frac{\ln(\rho_{ij}\delta_i\delta_j + 1)}{\sqrt{\ln(1 + \delta_i^2)\ln(1 + \delta_j^2)}} \quad (i, j = 1, \dots, N_s) \quad (5)$$

where  $\rho_{ij}$  is the cross-correlation coefficient between variables  $X_i$  and  $X_j$  in the  $X$  space;  $\delta_i$  and  $\delta_j$  are the coefficients of variation of variables  $X_i$  and  $X_j$ , respectively.

After obtaining the cross-correlation coefficient matrix  $\rho_0$  and the autocorrelation coefficient matrix  $\rho_{Ak}$ , their lower triangular matrix  $L_1$  and  $L_{2k}$  can be derived by Cholesky decomposition:  $L_1L_1^T = \rho_0$ ,  $L_{2k}L_{2k}^T = \rho_{Ak}$ . And then, the discretized random field  $H_k^Y$  can be generated using the following equation:

$$H_k^Y(x, y) = L_{2k}UL_1^T \quad (k = 1, \dots, N_s) \quad (6)$$

where  $(x, y)$  is the spatial position of discrete points.

- (3) Correlated non-normal space ( $X$  space): The discretized random

field  $H_k$  can be obtained by the isoprobabilistic transformation by Eq. (7):

$$H_k(x, y) = F^{-1}\{\Phi[H_k^Y(x, y)]\} \quad (k = 1, \dots, N_s) \quad (7)$$

where  $F^{-1}(\cdot)$  is inverse of the cumulative distribution function of non-normal distribution function  $F$ ; and  $\Phi(\cdot)$  is the cumulative distribution function of standard normal distribution. If the random variables are lognormally distributed, the appropriate lognormal random fields can be obtained by exponentiating the corresponding Gaussian field as follows:

$$H_k(x, y) = \exp(\mu_{\ln X_k} + \sigma_{\ln X_k} H_k^Y(x, y)) \quad (k = 1, \dots, N_s) \quad (8)$$

where  $\mu_{\ln X_k}$  and  $\sigma_{\ln X_k}$  are the mean and the standard deviation of the logarithm of variable  $X_k$  and they can be calculated by Eqs. (9a) and (9b), respectively (Babu and Murthy, 2005; Cho, 2012; Ahmed, 2009; Zhu et al., 2013):

$$\sigma_{\ln X} = \sqrt{\ln(1 + \delta_X^2)} = \sqrt{\ln(1 + (\sigma_X/\mu_X)^2)} \quad (9a)$$

$$\mu_{\ln X} = \ln(\mu_X/\sqrt{1 + \delta_X^2}) = \ln \mu_X - \frac{1}{2}\sigma_{\ln X}^2 \quad (9b)$$

where  $\delta_X$  is the coefficient of variation of variable  $X$ .

### 3.3. Logarithmic translation

Some soil parameters have lower limits larger than zero. For example, SWCC parameter  $n$  should be larger than 1.0 to ensure SWCC parameter  $m$  is positive. The generation of a lognormal variable with a lower limit can be performed by logarithmic translation (Phoon et al., 2010).

The probability density function of a lognormal variable  $X$  is:

$$f(x) = \frac{1}{x\sigma_{\ln X}\sqrt{2\pi}} \exp\left(\frac{-(\ln x - \mu_{\ln X})^2}{2\sigma_{\ln X}^2}\right) \quad (10)$$

If the lognormal variable  $X$  has a lower bound  $A$ , a translation of variable  $X$ ,  $X' = X - A$ , could be conducted. Similar to Eq. (10), the probabilistic density function of the translation variable  $X'$  can be

written as:

$$f(x') = f(x - A) = \frac{1}{(x - A)\sigma_{\ln X'}\sqrt{2\pi}} \exp\left(\frac{-(\ln(x - A) - \mu_{\ln X'})^2}{2\sigma_{\ln X'}^2}\right) \tag{11}$$

where  $\mu_{\ln X'}$  and  $\sigma_{\ln X'}$  are the mean and standard deviation of the logarithm of variable  $X'$ , respectively. Similar to Eqs. (9a) and (9b),  $\mu_{\ln X'}$  and  $\sigma_{\ln X'}$  can be expressed by Eqs. (12a) and (12b), respectively.

$$\sigma_{\ln X'} = \sqrt{\ln\left(1 + \left(\frac{\sigma_X}{\mu_X - A}\right)^2\right)} \tag{12a}$$

$$\mu_{\ln X'} = \ln(\mu_X - A) - \frac{1}{2}(\sigma_{\ln X'})^2 \tag{12b}$$

Therefore, if variable  $X$  is a lognormal variable with lower bound  $A$ , random realizations of the normal variable  $\ln X' = \ln(X - A)$  can be generated first, with the mean of  $\mu_{\ln X'}$  and standard deviation of  $\sigma_{\ln X'}$ . Therefore, random realizations of variable  $X$  can be obtained by exponentiating the corresponding normal variable  $\ln X' = \ln(X - A)$  as follows:

$$X = \exp(\ln X') + A \tag{13}$$

### 4. Analyses and results

#### 4.1. The application-problem and boundary conditions

A two-dimensional dam model adopted in this study is shown in Fig. 2. The height of the dam is 13.7 m and the width of dam crest is 4 m. The upstream and downstream side slopes are 1V:3H and 2V:5H, respectively. The thickness of the dam foundation is 3.7 m and the initial water table coincides with the surface of the dam foundation. The upstream water table is assumed to rise to 11.7 m rapidly, and the saturated-unsaturated seepage in the dam considering the spatial variability of soil parameters is analyzed. The finite difference code FLAC (Itasca, 2006) is adopted for performing the saturated-unsaturated seepage analysis.

Initially, soil in the embankment is unsaturated. The initial hydrostatic water pressure varies linearly with the vertical distance from the water table, with positive pressure under the water table and negative pressure above the water table. The initial pore air pressure is assumed to be zero. The water head on the upstream boundary beneath the water table is fixed and the soil above the water table is permeable to gas. The downstream boundary is treated as seepage boundary. The bottom boundary is impervious.

As described in Section 2, the uncertainty of hydraulic conductivity of fluid phases is characterized by the uncertainty of two SWCC parameters ( $a$ ,  $n$ ) and the saturated hydraulic conductivity parameter ( $k_s$ ). Many authors reported that the three hydraulic parameters  $a$ ,  $n$  and  $k_s$  were lognormally distributed, and parameters  $a$  and  $n$  were negatively correlated (Botros et al., 2009; Phoon et al., 2010; Wang et al., 2015). Therefore, the three hydraulic parameters  $a$ ,  $n$  and  $k_s$  are assumed as correlated lognormal random fields, denoted herein as  $X_1$ ,  $X_2$ , and  $X_3$

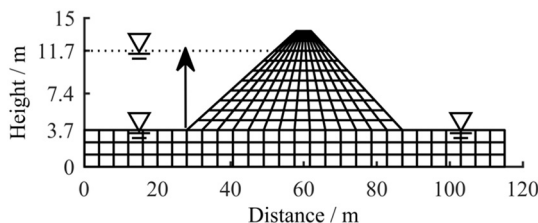


Fig. 2. Problem geometry and boundary conditions.

(see Table 1), and the cross-correlation coefficient between parameter  $a$  and  $n$  is  $-0.25$ . Because the variation in the hydraulic parameters is influenced by many factors, different values are reported for the COVs of these parameters. However, it is generally acknowledged that the COV of SWCC parameter  $n$  is smaller than that of parameter  $a$ , and the COV of saturated hydraulic conductivity  $k_s$  is relatively large (Botros et al., 2009; Dou et al., 2014). Although an isotropic autocorrelation structure was often assumed in previous studies (Srivastava et al., 2009; Le et al., 2012; Zhu et al., 2013), autocorrelations in the vertical direction tend to have much shorter distances than those in the horizontal direction (Ahmed, 2009; Gui et al., 2000; Cho, 2012). Based on laboratory tests (Li, 2017), different autocorrelation distances are assumed for vertical and horizontal directions, and the statistical values of the three random fields ( $X_1$ ,  $X_2$ , and  $X_3$ ) are presented in Table 1.

For the mean values listed in Table 1, the corresponding SWCC and hydraulic conductivity curves are shown in Fig. 3(a) and (b), respectively.

#### 4.2. Deterministic analysis

Prior to the seepage analysis considering spatial variability of hydraulic parameters, a deterministic analysis with mean input parameters is conducted to study the seepage behavior in the dam. A seepage section is defined to represent the relationship between suction and depth, and to represent the variation of flow rate with time. In Fig. 4(a), the vertical dotted line at the middle of the dam represents Section I and the sloping dashed line represents water table during the seepage.  $Q_u$ ,  $Q_s$  and  $Q_f$  are flow rates that pass through Section I in the unsaturated zone of dam body (above the water table), the saturated zone of dam body (below the water table) and dam foundation, respectively. The flow rate across Section I is calculated by adding the nodal flow along this section, which can be seen more clearly from the mesh and contour of node water pressure by FLAC in Fig. 4(b).

##### 4.2.1. Variation of suction with depth and time

The suction-depth relationship at different seepage times through Section I is shown in Fig. 5. The lower parts of the first four lines (e.g., 1–5 d) move leftwards gradually, while the upper parts of these lines remain nearly unchanged. It means that in the initial stage of seepage, the suction of the lower part of the dam body reduces with time, while the suction of the top part of the dam body remains unchanged. After 5 days of seepage from upstream to downstream of the dam, the flow begins to influence the top part of the dam. Thus, the upper parts of suction-depth curves in Fig. 5 begin to move left, which means that the suction of the top part of the dam begins to reduce. The suction-depth curves of the 30 d, 60 d and 90 d are very close in Fig. 5, which means the flow process becomes nearly stable after 30 days of seepage.

##### 4.2.2. Variation of water table with time

Except for the suction-depth curves on a vertical section, the saturated-unsaturated seepage process can also be expressed by the migration of water table (Fig. 6). The differences of water tables at different seepage times are significant in the initial stage of seepage. With the increase of seepage time, the water tables become close gradually. The water tables of the 30, 60 and 90 days are very close, which confirms that the flow process becomes nearly stable after 30 days of seepage. In this case study, all the phreatic surfaces pass the intersection point between the downstream dam slope and the dam foundation. Our trial computation demonstrates that the phreatic surfaces can also intersect the dam surface at a higher position if the saturated hydraulic conductivity becomes larger.

##### 4.2.3. Variation of flow rate with time

Flow rate is of conventional interest in seepage studies, as it indicates the amount of water loss through the dam. The variation of flow

**Table 1**  
Statistical properties of soil parameters.

Parameters	Random field	Mean ( $\mu$ )	Coefficient of variation (COV, or $\delta$ )	Vertical autocorrelation distance ( $L_v$ )	Horizontal autocorrelation distance ( $L_h$ )
$\alpha$	$X_1$	50 kPa	0.4	2 m	20 m
$n$	$X_2$	1.5	0.2	2 m	20 m
$k_s$	$X_3$	51.84 mm/d	0.6	2 m	20 m

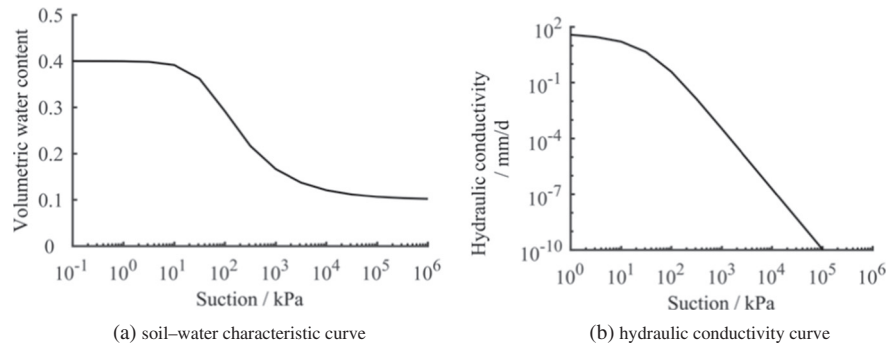


Fig. 3. Soil property functions for the mean value of hydraulic parameters.

rate through Section I with seepage time is shown in Fig. 7. In general, the flow rates of  $Q_u$ ,  $Q_s$  and  $Q_f$  increase initially and then decrease and tend to become steady after about 30 days of seepage. In the initial stage of seepage, the flow rate in the unsaturated zone and the saturated zone of the dam body ( $Q_u$  and  $Q_s$ , respectively) increase at nearly the same speed, while the flow rate in the dam foundation ( $Q_f$ ) increases more rapid than those of  $Q_u$  and  $Q_s$ . And the maximum value of  $Q_f$  is bigger than those of  $Q_u$  and  $Q_s$ . The reason is that  $Q_f$  is the flow rate in the dam foundation which is saturated all the time. And the hydraulic conductivity of unsaturated soil increases with the increase of water content, which can be seen from Fig. 3. However, after some time of seepage, the flow rates of  $Q_u$ ,  $Q_s$  and  $Q_f$  begin to decrease and gradually become steady. After about 30 days of seepage,  $Q_u$  reaches a steady value, and  $Q_s$  and  $Q_f$  are nearly close to their steady values. As shown in Fig. 6, with the increase of seepage time, the water table moves to the upper right direction. Therefore, the flow rate in the saturated zone of the dam body ( $Q_s$ ) becomes larger than the flow rate in the saturated zone of dam foundation ( $Q_f$ ). It should be mentioned that although the stable value of  $Q_u$  is smaller than those of  $Q_s$  and  $Q_f$ , the stable value of  $Q_u$  is not small enough to be neglected. After about 30 days of seepage, the ratio of  $Q_u$  to the summation of  $Q_u$  and  $Q_s$  is about 20%, which means that about 20% of water flow in the unsaturated zone through Section I of the dam body. Therefore, the flow rate is underestimated in the traditional seepage analysis which ignores water flow in the unsaturated zone.

Based on the above analysis, a seepage period of 30 days is adopted in the following stochastic simulations.

4.3. Stochastic simulations

In stochastic simulations, the suction distribution, position of water table and flow rate will be different from those of the deterministic

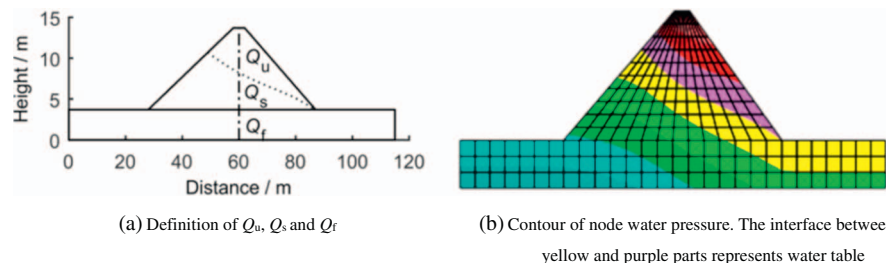


Fig. 4. Definition of section and flow rate. (For interpretation of the references to colour in this figure legend, the reader is referred to the web version of this article.)

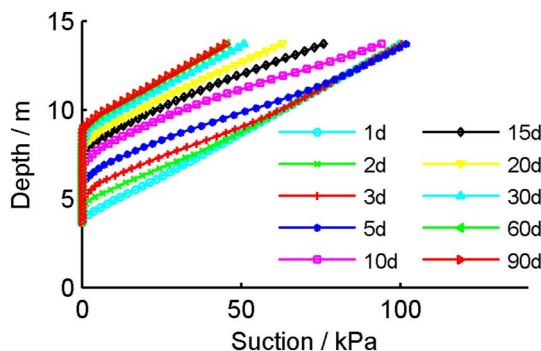


Fig. 5. Variation of suction with depth and time.

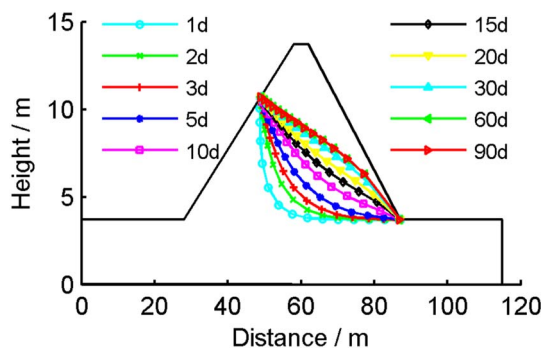


Fig. 6. Migration of water table in homogeneous dam.

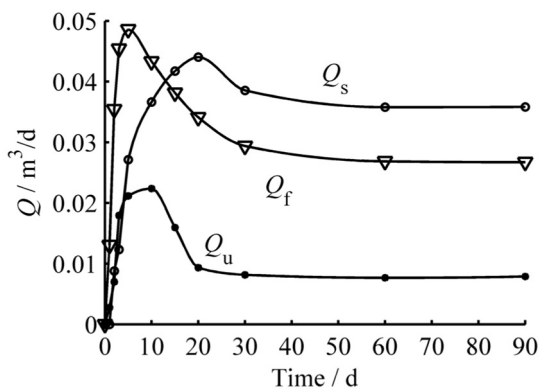


Fig. 7. Variation of flow rate with time.

analysis due to spatial variability of hydraulic variables. Considering the limitation of the length of this paper, only the flow rates of the unsaturated zone and the saturated zone through Section I of the dam body ( $Q_u$  and  $Q_s$ ) are illustrated in this section.

The stochastic approach for obtaining the statistical response of flow rate is performed by Monte Carlo simulation method (MCSM) combined with finite difference method. In Monte Carlo simulation, a series of random fields are generated in a manner consistent with their probability distribution and correlation structure, and each set of discrete values are considered as input soil parameters for each Monte Carlo simulation. The process must be repeated many times so that the estimated values such as the mean, standard deviation and probability density functions of flow rates are not influenced by the occurrence of extremely large or small events. Since the increase in number of simulations also increases the computational efforts, a compromise between accuracy and computational time should be achieved by convergence analysis.

To perform Monte Carlo Simulation of the seepage in the dam, a MATLAB function and a FISH (the built-in programming language of FLAC) function were written. The MATLAB function was used to generate various groups of discretized data for each random field. The discretized data are then read into the FLAC code by the FISH function, which was used to run the Monte Carlo Simulation.

4.3.1. Convergence analysis

4.3.1.1. Discretization of random fields. As mentioned in Section 4.1, hydraulic parameters  $a$ ,  $n$  and  $k_s$  are considered as lognormal distributed random fields, and the midpoint discretization method is used for generating the random fields of  $a$ ,  $n$  and  $k_s$ . A lower limit of 1.05 for parameter  $n$  is defined for ensuring a positive value of SWCC parameter  $m$ . Results of a sample realization of the discretization of the three random fields are shown in Fig. 8. The histograms represent relative frequency distributions of the discrete data for all the discrete points, and the curves represent the fitted lognormal probability distribution functions. Note that the frequency distribution of the discrete data does not fit lognormal distribution very well. Furthermore, according to mathematical statistics, the means of the

three groups of discrete data of random fields  $a$ ,  $n$  and  $k_s$  are 45.15, 1.45 and 42.18, respectively, and the corresponding coefficients of variation are 0.32, 0.14 and 0.48, respectively. Obviously, these values are not consistent with the means and coefficients of variation shown in Table 1.

However, with the increase of the number of realizations of the discretization of random fields, the relative frequency distribution of the discrete data tends to meet the target lognormal distribution very well. Fig. 9 shows the histograms of generated parameters  $a$ ,  $n$  and  $k_s$  together with the fitted lognormal distribution functions for 100 realizations. Agreement between the frequency distribution of the discrete data and the fitted lognormal functions is very good. The means of the 100 discrete data sets for random fields  $a$ ,  $n$  and  $k_s$  are 49.95, 1.50 and 51.72, respectively, and the corresponding coefficients of variation are 0.39, 0.21 and 0.59, respectively. These statistical values are very close to the corresponding values shown in Table 1. Therefore, 100 realizations of the discretization of random fields are sufficient for representing the statistics of random fields  $a$ ,  $n$  and  $k_s$ . It should be mentioned that all the discrete data of parameter  $n$  are larger than 1.05, which is shown by the histogram in Fig. 9(b). This is benefited from the logarithm translation algorithm for parameter  $n$ .

4.3.1.2. Probability distribution of flow rate. To analyze the characteristic of flow rates  $Q_u$  and  $Q_s$  more clearly, the probability density functions  $Q_u$  and  $Q_s$  at different seepage times are shown in Fig. 10(a) and (b), respectively, and the probability density functions of ratio  $Q_r$  ( $Q_r = Q_u / (Q_u + Q_s)$ ) are shown in Fig. 10(c). It can be seen that the distribution of flow rates  $Q_u$  and  $Q_s$  is lognormally distributed. The probability density curves of flow rate  $Q_u$  are very close to each other after 20 days of seepage (Fig. 10(a)). In Fig. 10(b), the modes of the lognormal distribution curves increase and the peaks of the lognormal distribution curves decrease with time during the 30 days of seepage. The curves tend to be closer and closer with increase in seepage time. Fig. 10(a)–(b) demonstrates that the seepage in the unsaturated zone of the dam body has become stable, and the seepage in the saturated zone of the dam body tends to be stable after 30 days of seepage.

Fig. 10(c) shows that the modes and peaks of the probabilistic curves of  $Q_r$  decrease and increase with seepage time, respectively. The stable value of the mode of  $Q_r$  is about 0.25, and many values of  $Q_r$  are larger than 0.25. In other words, water flow in the unsaturated zone about water table of the dam body accounts for about 25% of the total flow of the dam body. Neglecting the unsaturated flow in dam body will lead to underestimation of water flow.

4.3.2. Influence factors on flow rate

In the stochastic analysis with consideration of spatial variability of soil parameters, the flow rate of  $Q_u$  and  $Q_s$  will be influenced by the coefficient of variation (COV) and the autocorrelation distance of soil parameters. To analyze the influence of COV and autocorrelation distance on flow rate, four values of COVs (0.2, 0.4, 0.6, and 0.8) and five values of horizontal autocorrelation distances ( $L_h$ ) are considered (5, 10, 20, 100, and 1000 m). These values can represent the normal range

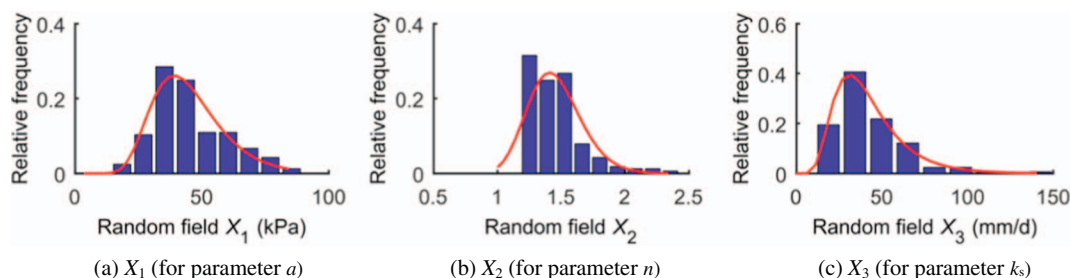


Fig. 8. Histogram of a sample realization of random field together with fitted lognormal distribution function.

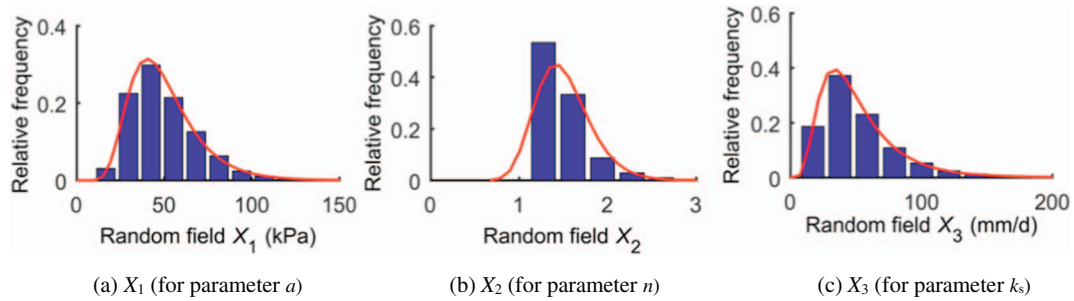


Fig. 9. Histogram of 100 realizations of random fields together with fitted lognormal distribution function

of COVs and autocorrelations of hydraulic parameters (Ahmed, 2009; Botros et al., 2009; Srivastava et al., 2009; Gui et al., 2000; Phoon et al., 2010; Le et al., 2012; Cho, 2012; Zhu et al., 2013; Dou et al., 2014; Wang et al., 2015). The means, coefficients of variations and autocorrelation distances listed in Table 1 are considered as reference values. To carry out the sensitivity analysis, different combinations of COV and  $L_h$  are considered. In each combination, only one value is changed (which is highlighted in bold letters in Table 2), and the other values are set to be their reference values. In general, the COVs of different parameters are different, but the autocorrelation distances of different parameters are the same. Thus, there are 12 combinations of COVs for the three parameters of  $a$ ,  $n$  and  $k_s$ . It can be seen from Table 2 that the combinations of COVs of No. 2, No. 5 and No. 11 are the same. Thus, there are only 10 independent combinations of COVs. For each group of COVs, three values of  $L_h$  (5, 20, and 1000 m) are considered, respectively. Besides, for No. 2 combination of COVs, two other values of  $L_h$  (10 and 100 m) are also adopted in the sensitivity analysis. Thus, altogether there are 32 independent combinations of COVs and autocorrelation distances. For each combination of parameters, 100 groups of random field simulations are conducted and the simulation period for each computation is 30 days for the balance of computing accuracy and efficiency.

4.3.2.1. Effects of coefficient of variation of hydraulic parameters on mean flow rate. Variation of mean flow rate ( $\mu(Q_u)$  and  $\mu(Q_s)$ ) with seepage time and different coefficients of variation of parameters ( $\delta_a$ ,  $\delta_n$ , and  $\delta_{k_s}$ ) are shown in Figs. 11 and 12.

As seen in Figs. 11 and 12, COVs of hydraulic parameters  $a$ ,  $n$ , and  $k_s$  affect the mean flow rates of both the unsaturated zone and saturated zone. The mean flow rates ( $\mu(Q_u)$  and  $\mu(Q_s)$ ) decrease with the increase in COVs of  $a$ ,  $n$ , and  $k_s$ . Among the three parameters, the COV of parameter  $n$  affects  $\mu(Q_u)$  and  $\mu(Q_s)$  greatly, while the COVs of parameter  $a$  and  $k_s$  affect  $\mu(Q_u)$  and  $\mu(Q_s)$  very slightly.

On the other hand, the value of  $\mu(Q_u)$  increases with time for the first 25 days and then  $\mu(Q_u)$  begins to decrease. However, the value of  $\mu(Q_s)$  keeps increasing during the 30 days of seepage simulation, and a steady tendency can be predicted reasonably from these curves. This characteristic is similar to that of Fig. 10, which can be found from the variation of curves with time.

The horizontal autocorrelation distance  $L_h$  is assumed to be 20 m in Figs. 11 and 12. Similar results can be found with different  $L_h$  values (such as 10 m or 1000 m), although they are not presented herein. Similar relationship between mean flow rates and COVs was obtained by Griffiths and Fenton (1993) and Srivastava et al. (2009) in their study on seepage in spatially random soil. The decrease in flow rates with the increase of COVs of hydraulic parameters is an important observation from the point of view of design. The traditional design method may rely on this variability to reduce flow rates on average.

4.3.2.2. Effects of coefficient of variation of hydraulic parameters on coefficient of variation of flow rate. Variation of the COVs of flow rates ( $\delta(Q_u)$  and  $\delta(Q_s)$ ) with seepage time ( $T$ ) and different COVs of hydraulic parameters ( $\delta_a$ ,  $\delta_n$ , and  $\delta_{k_s}$ ) are shown in Figs. 13 and 14. Because the mean flow rate  $\mu(Q_s)$  is zero at  $T = 5$  d (Fig. 12), the COV of  $Q_s$  at  $T = 5$  d is infinite, and they are not shown in Fig. 14. The horizontal autocorrelation distance is set to be 20 m for Figs. 13 and 14. Similar results can be found with different  $L_h$  values (such as 10 m or 1000 m), although they are not presented herein.

Figs. 13 and 14 indicate that COVs of parameters  $a$ ,  $n$ , and  $k_s$  affect COVs of both the unsaturated zone ( $Q_u$ ) and the saturated zone ( $Q_s$ ). The COVs of flow rate ( $\delta(Q_u)$  and  $\delta(Q_s)$ ) increase with the increase of COVs of  $a$ ,  $n$ , and  $k_s$ . The COV of parameter  $n$  affects  $\delta(Q_u)$  and  $\delta(Q_s)$  greatly, while the COV of parameter  $a$  barely affects  $\delta(Q_u)$  and  $\delta(Q_s)$ . The influence of the COV of  $k_s$  is moderate among the three parameters. However, the variation of  $\delta(Q_u)$  and  $\delta(Q_s)$  with time is different from that of  $\mu(Q_u)$  and  $\mu(Q_s)$ . The values of  $\delta(Q_u)$  and  $\delta(Q_s)$  decrease with increasing seepage time, which means the seepage tends to be stable with increase in time.

Comparing Figs. 13 and 14 with Table 2, it can be seen that the values of  $\delta(Q_u)$  and  $\delta(Q_s)$  are much larger than those of  $\delta_a$ ,  $\delta_n$  and  $\delta_{k_s}$ , and  $\delta(Q_u)$  is larger than  $\delta(Q_s)$ . This means that the seepage, especially in the unsaturated zone, varies greatly due to the variability of hydraulic parameters. The traditional deterministic approach does not reflect the variability of saturated-unsaturated seepage. A stochastic modeling approach must be used to account for this variability.

4.3.2.3. Effects of horizontal autocorrelation distance of hydraulic parameters on mean flow rate. Variations of mean of flow rates ( $\mu(Q_u)$

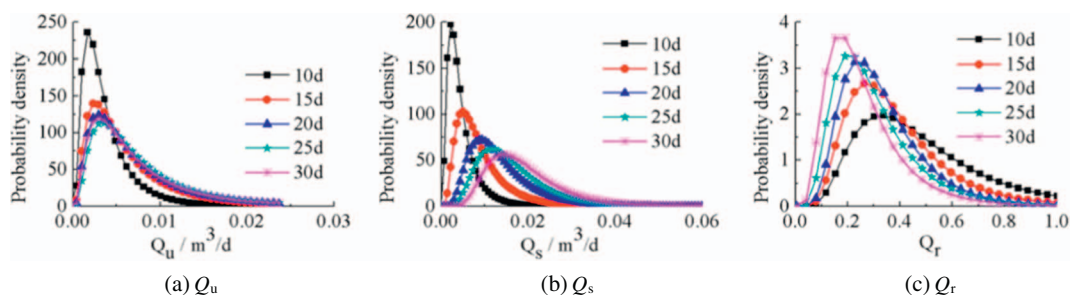
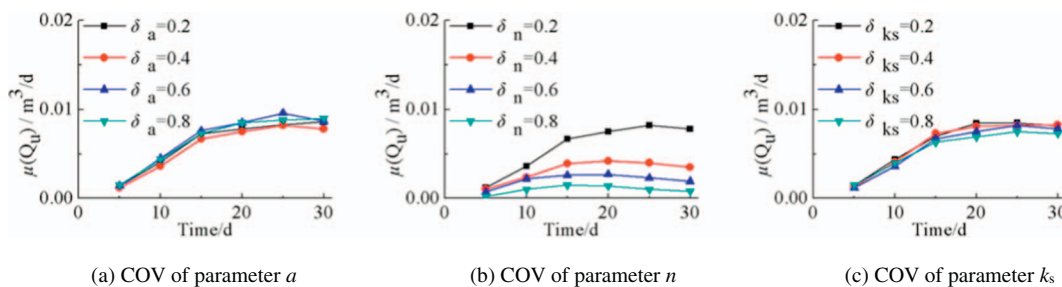


Fig. 10. Probability density functions (PDFs) of flow rate at different seepage times.

**Table 2**  
Combinations of coefficients of variation and autocorrelation distances.

No.		1	2	3	4	5	6	7	8	9	10	11	12
Coefficient of variation (COV, or $\delta$ )	$\delta_a$	0.2	0.4	0.6	0.8	0.4	0.4	0.4	0.4	0.4	0.4	0.4	0.4
	$\delta_n$	0.2	0.2	0.2	0.2	0.2	0.4	0.6	0.8	0.2	0.2	0.2	0.2
	$\delta_{ks}$	0.6	0.6	0.6	0.6	0.6	0.6	0.6	0.6	0.2	0.4	0.6	0.8
Autocorrelation distance	$L_{h1}/L_{h3}/L_{h5}$	5/20/1000 m (Calculated for each group of COVs)											
	$L_{h2}$	10 m (Calculated only for COV No. 2)											
	$L_{h4}$	100 m (Calculated only for COV No. 2)											



**Fig. 11.** Variation of mean flow rate  $\mu(Q_u)$  with seepage time and COVs of parameters.

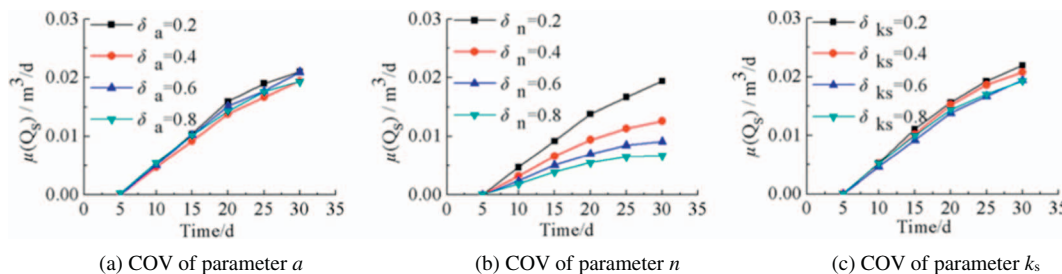


**Fig. 12.** Variation of mean flow rate  $\mu(Q_s)$  with seepage time and COVs of parameters.

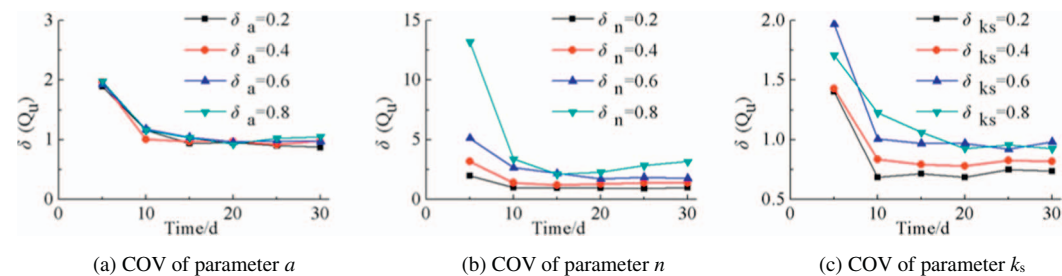


**Fig. 13.** Variation of COV of flow rate  $\delta(Q_u)$  with seepage time and COVs of parameters.

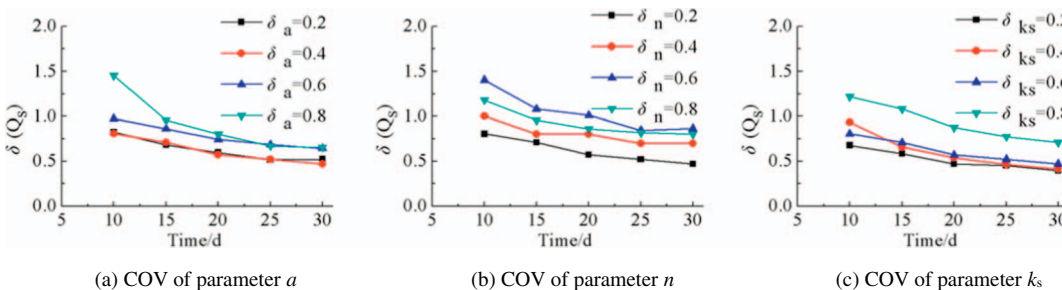


**Fig. 14.** Variation of COV of flow rate  $\delta(Q_s)$  with seepage time and COVs of parameters.

and  $\mu(Q_s)$  with seepage time and different horizontal autocorrelation distances ( $L_h$ ) of soil parameters are shown in Fig. 15, with the COVs of three hydraulic parameters set to their reference values. It is evident that  $L_h$  affects  $\mu(Q_u)$  greatly. A large value of  $L_h$  leads to a large value of

$\mu(Q_u)$ , and the difference of  $\mu(Q_u)$  of different  $L_h$  increases with time. A reasonable explanation is that a realization of random field with higher autocorrelation distance tends to have more elements of similar properties close together, which in turn implies that the most

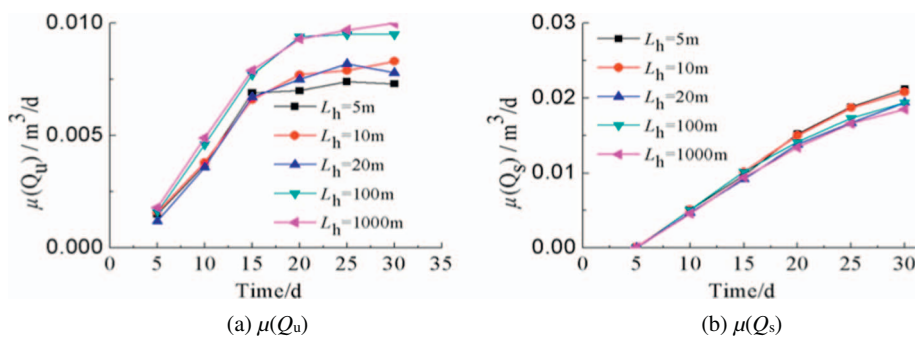


Fig. 15. Variation of mean of flow rate with seepage time and autocorrelation distance.

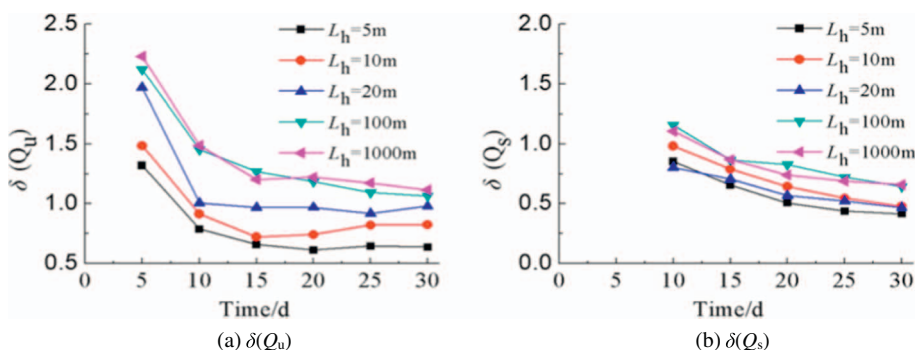


Fig. 16. Variation of coefficient of variation of flow rate with seepage time and autocorrelation distance.

permeable paths are likely to be less tortuous and water can flow through these elements easier. However, the influence of  $L_h$  on  $\mu(Q_s)$  is very small. Therefore, not considering the spatial variability of soil parameters has little influence on the estimation of flow rate in the saturated zone, but it will lead to overestimation of flow rate in the unsaturated zone. This conclusion is consistent with the study by Ahmed (2009).

4.3.2.4. Effects of horizontal autocorrelation distance of hydraulic parameters on coefficient of variation of flow rate. Variations of the COVs of flow rates ( $\delta(Q_u)$  and  $\delta(Q_s)$ ) with seepage time and different horizontal autocorrelation distances ( $L_h$ ) of soil parameters are shown in Fig. 16, with the COVs of three hydraulic parameters set to their reference values. Similar to Fig. 14, the COVs of  $Q_s$  at  $T = 5$  d are not shown in Fig. 16(b). As can be seen, although  $L_h$  values have little influence on  $\mu(Q_s)$ , they affect  $\delta(Q_s)$  greatly. Increasing values of  $L_h$  corresponds to increasing values of  $\delta(Q_u)$  and  $\delta(Q_s)$ . In the traditional probabilistic method, spatial variability of soil parameters is not considered, which in fact assumes that the autocorrelation distance is infinite (Jimenez and Sitar, 2009). In reality, the correlation lengths of soil parameters are usually short. Therefore, the variability of flow rate is overestimated in the traditional probabilistic methods.

### 5. Conclusions

Spatial variability of soil parameters affects seepage behavior of earth dams. This paper combines Monte Carlo simulation, random field theory and finite difference modeling to analyze the effect of spatial variability of hydraulic parameters on saturated-unsaturated seepage behavior in an earth dam. The van Genuchten model is adopted for representing soil-water characteristic curve (SWCC). The SWCC parameters ( $\alpha$  and  $n$ ) and saturated hydraulic conductivity ( $k_s$ ) are considered as cross-correlated lognormal random fields. The midpoint method is adopted for discretizing random fields, and logarithmic translation is used for generating lognormal variable with a lower limit.

In order to investigate the influence of coefficients of variation (COVs) and the horizontal autocorrelation distance ( $L_h$ ) of hydraulic parameters on the flow rate in the dam body, four values of COVs and

five values of  $L_h$  are assumed for the three hydraulic parameters ( $\alpha$ ,  $n$ ,  $k_s$ ). The results indicate that the water flow in unsaturated zone above water table should not be neglected for the accurate analysis of seepage behavior, and the uncertainties of three hydraulic parameters have great influence on the flow rate.

When the autocorrelation distances of hydraulic parameters are fixed, the increase in COVs of hydraulic parameters leads to decrease in mean flow rates in both unsaturated zone ( $Q_u$ ) and saturated zone ( $Q_s$ ) of dam body, but leads to increase in the COVs of flow rates  $Q_u$  and  $Q_s$ . Among the three hydraulic parameters, parameter  $n$  affects the mean and COV of flow rate greatly, while parameter  $\alpha$  affects the mean and COV of flow rate slightly.

When the COVs of hydraulic parameters are fixed, the mean flow rate  $\mu(Q_u)$  and the COVs of both  $Q_u$  and  $Q_s$  increase with horizontal autocorrelation distance, but the mean flow rate  $\mu(Q_s)$  remains nearly unchanged. Not considering the spatial variability of hydraulic parameters will lead to overestimation of mean and COV of flow rate in the dam body. This observation is very useful in design of dams.

It can be found that the influence of COVs of hydraulic parameters  $n$  and  $k_s$  on flow rate is greater than that of horizontal autocorrelation distance. More attention should be paid on accurate measuring of the COVs of hydraulic parameters  $n$  and  $k_s$  in engineering practices.

### Acknowledgements

The financial support from the National Natural Science Foundation, China (41572282, 41372281), the Natural Science Foundation of Anhui, China (JZ2015AKZR0045) and the China Scholarship Council (CSC) are greatly acknowledged. The first author wishes to acknowledge the Clemson University Center for Risk Engineering & System Analytics (RESA) for hosting her sabbatical leave at Clemson and the third author wishes to acknowledge the financial support of RESA Center during the period when the work was done.

### References

Ahmed, A.A., 2009. Stochastic analysis of free surface flow through earth dams. *Comput. Geotech.* 36 (7), 1186–1190. <http://dx.doi.org/10.1016/j.compgeo.2009.05.005>.

- Babu, G.L.S., Murthy, D.S.N., 2005. Reliability analysis of unsaturated soil slopes. *J. Geotech. Geoenviron.* 131 (11), 1423–1428. [http://dx.doi.org/10.1061/\(ASCE\)1090-0241\(2005\)131:11\(1423\)](http://dx.doi.org/10.1061/(ASCE)1090-0241(2005)131:11(1423)).
- Botros, F.E., Harter, T., Onsoy, Y.S., Tuli, A., Hopmans, J.W., 2009. Spatial variability of hydraulic properties and sediment characteristics in a deep alluvial unsaturated zone. *Vadose Zone J.* 8 (2), 276–289. <http://dx.doi.org/10.2136/vzj2008.0087>.
- Chan, C.L., Low, B.K., 2012. Practical second-order reliability analysis applied to foundation engineering. *Int. J. Numer. Anal. Methods Geomech.* 36 (11), 1387–1409. <http://dx.doi.org/10.1002/nag.1057>.
- Ching, J.Y., Phoon, K.K., 2013. Effect of element sizes in random field finite element simulations of soil shear strength. *Comput. Struct.* 126 (1), 120–134. <http://dx.doi.org/10.1016/j.compstruc.2012.11.008>.
- Cho, S.E., 2007. Effects of spatial variability of soil properties on slope stability. *Eng. Geol.* 92 (3), 97–109. <http://dx.doi.org/10.1016/j.enggeo.2007.03.006>.
- Cho, S.E., 2012. Probabilistic analysis of seepage that considers the spatial variability of permeability for an embankment on soil foundation. *Eng. Geol.* 133–134 (3), 30–39. <http://dx.doi.org/10.1016/j.enggeo.2012.02.013>.
- Cho, S.E., Lee, S.R., 2001. Instability of unsaturated soil slopes due to infiltration. *Comput. Geotech.* 28 (3), 185–208. [http://dx.doi.org/10.1016/S0266-352X\(00\)00027-6](http://dx.doi.org/10.1016/S0266-352X(00)00027-6).
- Dou, H.Q., Han, T.C., Gong, X.N., Zhang, J., 2014. Probabilistic slope stability analysis considering the variability of hydraulic conductivity under rainfall infiltration–redistribution conditions. *Eng. Geol.* 183, 1–13. <http://dx.doi.org/10.1016/j.enggeo.2014.09.005>.
- Fredlund, D.G., Houston, S.L., 2009. Protocol for the assessment of unsaturated soil properties in geotechnical engineering practice. *Can. Geotech. J.* 46 (6), 694–707. <http://dx.doi.org/10.1139/T09-010>.
- van Genuchten, M.T., 1980. A closed form equation for predicting the hydraulic conductivity of unsaturated soils. *Soil Sci. Soc. Am. J.* 44 (5), 892–898. <http://dx.doi.org/10.2136/sssaj1980.03615995004400050002x>.
- Griffiths, D.V., Fenton, G.A., 1993. Seepage beneath water retaining structures founded on spatially random soil. *Géotechnique* 43 (6), 577–587. <http://dx.doi.org/10.1680/geot.1993.43.4.577>.
- Gui, S.X., Zhang, R.D., Turner, J.P., Xue, X.Z., 2000. Probabilistic slope stability analysis with stochastic soil hydraulic conductivity. *J. Geotech. Geoenviron.* 126 (1), 1–9. [http://dx.doi.org/10.1061/\(ASCE\)1090-0241](http://dx.doi.org/10.1061/(ASCE)1090-0241).
- Itasca, 2006. Reference Manual, FLAC 5.0. Itasca Consulting Group Inc., Minneapolis.
- Ji, J., Liao, H.L., Low, B.K., 2012. Modeling 2-D spatial variation in slope reliability analysis using interpolated autocorrelations. *Comput. Geotech.* 40 (3), 135–146. <http://dx.doi.org/10.1016/j.compgeo.2011.11.002>.
- Jiang, S.H., Li, D.Q., Zhou, C.B., Phoon, K.K., 2014. Slope reliability analysis considering effect of autocorrelation functions. *Chin. J. Geotech. Eng.* 36 (3), 508–518. <http://dx.doi.org/10.11779/CJGE201403014>.
- Jimenez, R., Sitar, N., 2009. The importance of distribution types on finite element analyses of foundation settlement. *Comput. Geotech.* 36 (3), 474–483. <http://dx.doi.org/10.1016/j.compgeo.2008.05.003>.
- Juang, C.H., Lu, C.C., Hwang, J.H., 2009. Assessing probability of surface manifestation of liquefaction in a given exposure time using CPTU. *Eng. Geol.* 104, 223–231.
- Juang, C.H., Ching, J., Luo, Z., Ku, C.S., 2012. New models for probability of liquefaction using standard penetration tests based on an updated database of case histories. *Eng. Geol.* 133, 85–93.
- Juang, C.H., Wang, L., Hsieh, H.S., Atamturktur, S., 2014. Robust geotechnical design of braced excavations in clays. *Struct. Saf.* 49, 37–44. <http://dx.doi.org/10.1016/j.strusafe.2013.05.003>.
- Kim, J., Jeong, S., Regueiro, R.A., 2012. Instability of partially saturated soil slopes due to alteration of rainfall pattern. *Eng. Geol.* 147–148, 28–36.
- Le, T.M.H., Gallipoli, D., Sanchez, M., Wheeler, S.J., 2012. Stochastic analysis of unsaturated seepage through randomly heterogeneous earth embankments. *Int. J. Numer. Anal. Methods Geomech.* 36 (8), 1056–1076. <http://dx.doi.org/10.1002/nag.1047>.
- Li, P., 2017. Assessment of Spatial Variability of Unsaturated Clay in Hefei. Dissertation Hefei University of Technology.
- Li, W.X., Lu, Z.M., Zhang, D.X., 2009. Stochastic analysis of unsaturated flow with probabilistic collocation method. *Water Resour. Res.* 45 (8), 2263–2289. <http://dx.doi.org/10.1029/2008WR007530>.
- Lu, C.H., Hwang, J.H., Juang, C.H., Ku, C.S., Luo, Z., 2009. Framework for assessing probability of exceeding a specified liquefaction-induced settlement at a given site in a given exposure time. *Eng. Geol.* 108, 24–35.
- Nam, S., Gutierrez, M., Diplas, P., Petrie, J., Wayllace, A., Lu, N., Muñoz, J.J., 2009. Comparison of testing techniques and models for establishing the SWCC of riverbank soils. *Eng. Geol.* 110, 1–10. <http://dx.doi.org/10.1016/j.enggeo.2009.09.003>.
- Papaioannou, I., Straub, D., 2012. Reliability updating in geotechnical engineering including spatial variability of soil. *Comput. Geotech.* 42, 44–51. <http://dx.doi.org/10.1016/j.compgeo.2011.12.004>.
- Phoon, K.K., Santoso, A., Quek, S.T., 2010. Probabilistic analysis of soil-water characteristic curves. *J. Geotech. Geoenviron.* 136 (3), 445–455. [http://dx.doi.org/10.1061/\(ASCE\)GT.1943-5606.0000222](http://dx.doi.org/10.1061/(ASCE)GT.1943-5606.0000222).
- Qin, Q., Lin, D.J., Mei, G., 2006. Theory and Applications: Reliability Stochastic Finite Element Methods. Qinghua University Press, Beijing.
- Rahimi, A., Rahardjo, H., Leong, E.C., 2010. Effect of hydraulic properties of soil on rainfall-induced slope failure. *Eng. Geol.* 114 (3–4), 135–143.
- Sillers, W.S., Fredlund, D.G., 2001. Statistical assessment of soil-water characteristic curve models for geotechnical engineering. *Can. Geotech. J.* 38 (6), 1297–1313. <http://dx.doi.org/10.1139/t01-066>.
- Srivastava, A., Babu, G.L.S., Haldar, S., 2009. Influence of spatial variability of permeability property on steady state seepage flow and slope stability analysis. *Eng. Geol.* 110 (3–4), 93–101. <http://dx.doi.org/10.1016/j.enggeo.2009.11.006>.
- Stefanou, G., 2009. The stochastic finite element method: past, present and future. *Comput. Methods Appl. Mech. Eng.* 198 (9–12), 1031–1051. <http://dx.doi.org/10.1016/j.cma.2008.11.007>.
- Sudret, B., Kiureghian, A.D., 2002. Comparison of finite element reliability methods. *Probab. Eng. Mech.* 17 (4), 337–348. [http://dx.doi.org/10.1016/S0266-8920\(02\)00031-0](http://dx.doi.org/10.1016/S0266-8920(02)00031-0).
- Tan, X.H., Bi, W.H., Hou, X.L., Wang, W., 2011. Reliability analysis using radial basis function networks and support vector machines. *Comput. Geotech.* 38 (2), 178–186. <http://dx.doi.org/10.1016/j.compgeo.2010.11.002>.
- Tsagaras, I., Rahardjo, H., Toll, D.G., Leong, E.C., 2002. Controlling parameters for rainfall-induced landslides. *Comput. Geotech.* 29 (1), 1–27. [http://dx.doi.org/10.1016/S0266-352X\(01\)00019-2](http://dx.doi.org/10.1016/S0266-352X(01)00019-2).
- Vanmarcke, E.H., 1977. Probabilistic modeling of soil profiles. *J. Geotech. Eng.* 103 (11), 1227–1246.
- Wang, L., Hwang, J.H., Juang, C.H., Atamturktur, S., 2013. Reliability-based design of rock slopes — a new perspective on design robustness. *Eng. Geol.* 154, 56–63.
- Wang, Y.Q., Shao, M.A., Han, X.W., Liu, Z.P., 2015. Spatial variability of soil parameters of the van Genuchten model at a regional scale. *Clean* 43 (2), 271–278. <http://dx.doi.org/10.1002/clean.201300903>.
- Zhu, H., Zhang, L.M., Zhang, L.L., Zhou, C.B., 2013. Two-dimensional probabilistic infiltration analysis with a spatially varying permeability function. *Comput. Geotech.* 48 (4), 249–259. <http://dx.doi.org/10.1016/j.compgeo.2012.07.010>.